TISSUE ENGINEERING: Part A
Volume 20, Numbers 7 and 8, 2014

DOI: 10.1089/ten.tea.2013.0158

Linear Ordered Collagen Scaffolds Loaded with Collagen-Binding Basic Fibroblast Growth Factor Facilitate Recovery of Sciatic Nerve Injury in Rats

Fukai Ma, MS,[1,2] Zhifeng Xiao, PhD,[3] Bing Chen, PhD,[3] Xianglin Hou, MS,[3]
Jianwu Dai, PhD,[3,*] and Ruxiang Xu, PhD[1,2,*]

Natural biological functional scaffolds, consisting of biological materials filled with promoting elements, provide a promising strategy for the regeneration of peripheral nerve defects. Collagen conduits have been used widely due to their excellent biological properties. Linear ordered collagen scaffold (LOCS) fibers are good lumen fillers that can guide nerve regeneration in an ordered direction. In addition, basic fibroblast growth factor (bFGF) is important in the recovery of nerve injury. However, the traditional method for delivering bFGF to the lesion site has no long-term effect because of its short half-life and rapid diffusion. Therefore, we fused a specific collagen-binding domain (CBD) peptide to the N-terminal of native basic fibroblast growth factor (NAT-bFGF) to retain bFGF on the collagen scaffolds. In this study, a natural biological functional scaffold was constructed using collagen tubes filled with collagen-binding bFGF (CBD-bFGF)-loaded LOCS to promote regeneration in a 5-mm rat sciatic nerve transection model. Functional evaluation, histological investigation, and morphometric analysis indicated that the natural biological functional scaffold retained more bFGF at the injury site, guided axon growth, and promoted nerve regeneration as well as functional restoration.

Introduction

Peripheral nerve injury, which is often caused by accidents, tumor resection, congenital deformities, compression, or contusion, occurs in approximately 2.8% of trauma patients.[1] It may result in the partial or total loss of motor, sensory, and autonomic functions, and therefore have a marked negative impact on the quality of life.[2,3] Natural biological functional scaffolds, consisting typically of biological materials filled with promoting elements, have been developed to elicit axon regeneration after peripheral nerve injury. There have been several reports of their use to promote peripheral nerve repair.[4–9]

Collagen is one of the best characterized materials used in tissue engineering. Known for its low antigenicity, excellent biocompatibility, biodegradability, and bioresorbability, collagen is used widely for tissue regeneration.[10–13] In this study, collagen tubes were produced to serve as physical bridges to lesions between the proximal and distal stumps of disconnected nerves. Previous studies showed that nerve regeneration in a misdirected manner may result in loss of function.[14–16] We showed previously that linear ordered collagen scaffold (LOCS), another collagen material, has good nerve guidance properties.[17] In addition, LOCS can also be used to bind neurotrophic factors or as the backbone to construct drug delivery systems.[18,19]

The basic fibroblast growth factor (bFGF) plays an important role in promoting nerve regeneration. It has been reported that bFGF promotes neurite extension and stimulates Schwann cell proliferation *in vivo*.[20,21] The main sources of endogenous bFGF during regeneration are macrophages, Schwann cells, and sensory neurons.[22] However, the level of endogenous bFGF is insufficient for nerve regeneration, and simple delivery of exogenous bFGF is unsatisfactory because of its short half-life and rapid diffusion in the body fluids.[23,24] Previous studies showed that the collagen-binding domain (CBD) can bind to native collagen in a saturable manner.[25] Therefore, we fused CBD with native bFGF and constructed CBD-bFGF that showed notable collagen binding ability without impacting cytokine activity.[26] The CBD-bFGF was subsequently loaded onto a LOCS to control its release rate.

In this study, a natural biological functional scaffold consisting of collagen tubes and LOCS fibers loaded with CBD-bFGF was developed to bridge a 5-mm gap in the rat sciatic

[1]The Affiliated Bayi Brain Hospital, The Military General Hospital of Beijing PLA, Beijing, China.
[2]Graduate School, Southern Medical University, Guangzhou, China.
[3]State Key Laboratory of Trauma, Burns and Combined Injury, Chongqing Engineering Research Center for Nanomedicine, Institute of Combined Injury, College of Preventive Medicine, Third Military Medical University, Chongqing, China.
*These authors equally contributed to this work.

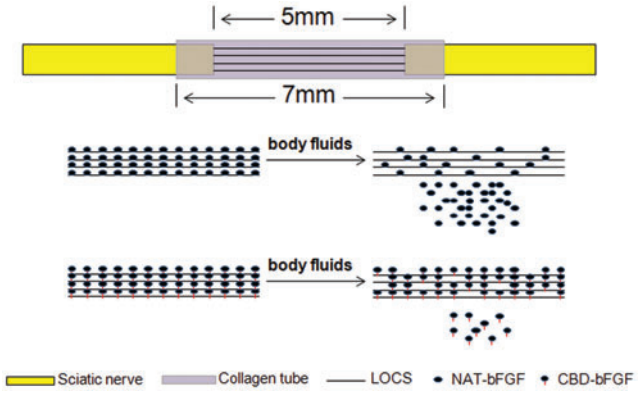

FIG. 1. Diagram of the natural biological functional scaffold and CBD-bFGF delivery system in the sciatic nerve transection model. CBD, collagen-binding domain; bFGF, basic fibroblast growth factor; LOCS, linear ordered collagen scaffold; NAT, native. Color images available online at www.liebertpub.com/tea

nerve. Native bFGF (NAT-bFGF), which exhibited similar biological activities but without the CBD, was also constructed (Fig. 1). An examination of regenerative outcome, including functional, morphological, and histological assessments, was carried out at 6 and 12 weeks after implantation.

Materials and Methods

Preparation of protein CBD-bFGF and NAT-bFGF

CBD-bFGF was prepared as described previously with simple modifications.[26] The gene encoding CBD-bFGF was amplified by polymerase chain reaction and inserted into the expression vector pET-28a. The constructed expression vector for bFGF with CBD (pET-CBD-bFGF) was transformed into *Escherichia coli* BL21 (DE3). The expression of the proteins was then induced by the addition of 1 mM isopropyl-β-D-thiogalactopyranoside (IPTG) at 25°C for 8 h. Nickel chelation chromatography (Amersham Biosciences) was then used to purify the targeted proteins from the supernatants. NAT-bFGF without CBD was also constructed in the same manner. The Bradford method was used to determine the protein concentration.[26]

Preparation of LOCS and collagen tubes

The LOCS derived from bovine aponeurosis was prepared as described previously.[17] Collagen tubes were derived from collagen membranes.[27] After scrolling on molds, collagen membranes were crosslinked by 1-ethyl-3-(3-dimethyl aminopropyl), carbodiimide (EDC) (30 mM), and N-hydroxysuccinimide (NHS) (10 mM) for 12 h. Then, the collagen tubes were washed using NaH_2PO_4 (0.1 M) and distilled water followed by freeze drying. The LOCS that 5 mm in length and collagen tubes 7 mm in length were sterilized by 8-kGy ^{60}Co irradiation (Fig. 2A, B). The LOCS was then loaded with 0.2 nmol of CBD-bFGF in 5 μL of distilled water, 0.2 nmol of NAT-bFGF in 5 μL of distilled water, or 5 μL of PBS 30 min before implantation.

Surgical procedure

Surgery was approved by the local authorities. The living conditions and experimental procedures were performed according to the National Institutes of Health Guide for the Care and Use of Laboratory Animals.

Male Sprague Dawley rats (200–220 g) were used in this study. All rats were randomized into the following three grafted groups and a normal group: nerve gap bridged by the collagen tube + LOCS + CBD-bFGF group ($n = 34$), nerve gap bridged by the collagen tube + LOCS + NAT-bFGF group ($n = 34$), nerve gap bridged by the collagen tube + LOCS + PBS group ($n = 34$), and normal rats ($n = 11$). Rats were anesthetized by intraperitoneal injection of sodium pentobarbital (40 mg/kg body weight). After exposure of the sciatic nerve on the right side, a segment 3 mm in length was transected to generate a defect 5 mm in length due to

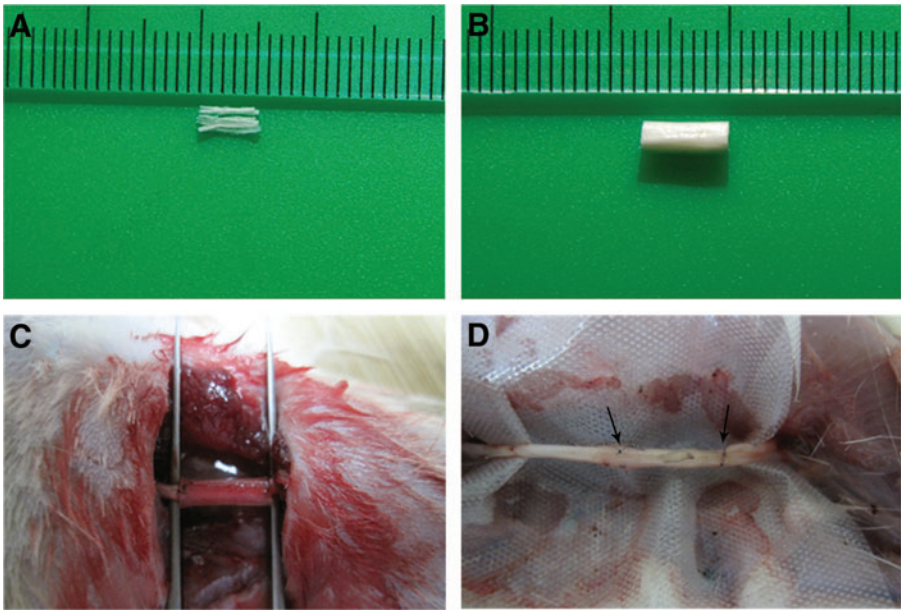

FIG. 2. The collagen scaffolds, surgical procedure, and regenerated nerve. **(A)** Photograph of the linear ordered scaffold. **(B)** Photograph of the collagen tube. **(C)** Photograph of the surgical procedure. The transected nerve was connected to the natural biological functional scaffold. **(D)** Photograph of the regenerating nerve cable at 12 weeks postimplantation. The arrows indicate the two ends of the regenerated nerve. Color images available online at www.liebertpub.com/tea

retraction of the nerve ends. Then, a collagen tube 7 mm in length (inner diameter 1.5 mm, outer diameter 2.0 mm) filled with a bundle of about 60 LOCS fibers (each about 50 μm in diameter and 5 mm in length) (Supplementary Fig. S1; Supplementary Data are available online at www.liebertpub.com/tea) carrying CBD-bFGF, NAT-bFGF, or PBS was sutured to the proximal and distal ends of the transected sciatic nerve using 9/0 monofilament nylon interrupted sutures (Fig. 2C). The muscle layers and skin were sutured with 4-0 sutures. Thirty-three animals at 6 weeks and 44 animals at 12 weeks post-transplantation were sacrificed by anesthetic overdose.

In vivo *bFGF binding assay*

At 1, 4, 7, and 10 days after implantation, three rats from each group were sacrificed at each time point, the LOCS were lysed with 200 μL of RIPA buffer (Sigma) supplemented with proteinase inhibitor cocktail (Roche Applied Science) for 30 min on ice. The supernatant was collected and measured using a human bFGF ELISA kit (Neo-Bioscience Technology Co., Ltd).

Walking track analysis

Walking track analysis was carried out each week after surgery to assess functional recovery, and the sciatic function index (SFI) value was calculated using the method proposed by Bain *et al*.[28] The process of walking track analysis was performed by the same investigator who was blinded to the group assignments. The footprints left on white paper were recorded to calculate the SFI value based on the following equation:

$$\mathrm{SFI} = -38.3 \times (\mathrm{EPL} - \mathrm{NPL})/\mathrm{NPL} + 109.5 \times (\mathrm{ETS} - \mathrm{NTS})/\mathrm{NTS} + 13.3 \times (\mathrm{EITS} - \mathrm{NITS})/\mathrm{NITS} - 8.8,$$

where PL is the distance between the third toe and heel, TS is the distance between the first and fifth toes, ITS is the distance between the second and fourth toes, EPL, ETS, and EITS are the distances (PL, TS, ITS) on the experimental (right) side, respectively, and NPL, NTS, and NITS are the distances (PL, TS, ITS) on the contralateral (left) side, respectively.

Electrophysiological evaluation

Twelve weeks after surgery, the rats were anesthetized as described above. After re-exposure of the regenerated sciatic nerve, a crook-shaped bipolar stimulating electrode was placed in the proximal end of the nerve, while two record electrodes were placed in the proximal and distal ends of the nerve, respectively. Nerve conduction velocity (NCV) and amplitude of the compound muscle action potential (ACMAP) were recorded by an electromyography system (RM6240; Chengdu Instrument Co.).

FG retrograde tracing

At week 10, the rats were sedated under conditional anesthesia. The sciatic nerve was re-exposed as described above, and 3 μL of 5% (5 mg/100 μL, dissolved in saline) retrograde fluorescent tracer Fluorogold (FG; Fluorochrome) was injected into the site 4 mm from coaptation of the distal end. After closing in layers, the rats were allowed to recover for 2 weeks. The rats were sacrificed at week 12; the dorsal root ganglion (DRG) at L4–L6 was dissected out and embedded in the optimal cutting temperature (O.C.T.) compound before freezing in liquid nitrogen. The DRG was cut into sections 10 μm thick on a freezing microtome and placed on glass slides for observation. Fluorescent neurons that exhibited a bright, golden color were counted under a fluorescence microscope (Carl Zeiss).

Histological investigation and morphometric analysis

At 6 and 12 weeks after implantation, the regenerating nerve cable at the injury site was harvested. After postfixing with 1% OsO_4, the distal end of the regenerated nerve was embedded in paraffin and cut into 5-μm transverse sections on a cryostat. After antigen retrieval, the sections were incubated with goat serum to block nonspecific immunoreactivity. Then, they were incubated with mouse anti-neurofilament (NF) 200 (1:100 dilution; Zeta Corp.) and anti-S-100 (1:100 dilution; Zeta Corp.) overnight at 4°C. Following a wash with PBS, sections were incubated with a secondary antibody (goat anti-mouse IgG; Invitrogen) for 10 min. After incubation with HRP-Streptavidin (Jackson Immuno Research), they were washed three times with PBS followed by incubation with DAB (Invitrogen) for 5 min. Finally, the sections were mounted with a resinous medium and observed under a light microscope (Nikon). At least three random photographs were taken per section. The percentages of NF and S-100 (positive staining area/total area) in each photograph were calculated using the Image-Pro Plus software (Media Cybernetics).

Luxol fast blue was used for staining of myelin. After deparaffinization and dehydration in 95% ethyl alcohol, sections of each specimen were left in the Luxol fast blue solution (Sigma) overnight at 37°C, excess stain was rinsed off, the sections were differentiated in the lithium carbonate solution and 70% ethyl alcohol, counterstained with Cresyl violet, the sections were differentiated in 95% ethyl alcohol, mounted with the resinous medium, and examined under a light microscope (Nikon). At least three photographs of random areas were taken per section. The number and diameter of the newly regenerating axons in each photograph were evaluated using the Image-Pro Plus software (Media Cybernetics).

The specimens were fixed in 2.5% glutaraldehyde, and postfixed with 1% OsO_4. After dehydration in increasing concentrations of acetone, the samples were embedded in epoxy resin to make ultrathin sections followed by staining with lead citrate and uranyl acetate. Finally, they were examined by transmission electron microscopy (TEM) (H-7650B; Hitachi). At least five photographs of random areas were taken per section. The Image-Pro Plus software was used to evaluate the thickness of the regenerated nerves in each photograph.

At week 12, the regenerating nerve cables were embedded in paraffin and cut into longitudinal sections 5 μm thick on a cryostat, and then stained with hematoxylin and eosin (HE) to visualize the structure.

Muscle mass ratio and Masson's trichrome staining

The weight ratio of the gastrocnemius muscles was measured 12 weeks post-transplantation. Immediately after

sacrifice, the bilateral gastrocnemius muscles were harvested and weighed on an electronic balance while still wet. The muscle mass ratio was calculated by dividing the muscle mass on the experimental side by that on the contralateral side. Subsequently, the midbelly of the muscle samples was subjected to Masson's trichrome staining. The percentage of muscle (positive staining area/total area) was calculated using the Image-Pro Plus software.

Statistical analysis

Statistical analyses were performed by one-way analysis of variance and the S-N-K *post hoc* test for multiple group comparisons using the SPSS 13.0 software (SPSS). The data are presented as mean ± SD. In all analyses, $p < 0.05$ was taken to indicate statistical significance (expressed as $^{*}p < 0.05$ or $^{**}p < 0.01$).

Results

General conditions of nerve grafting

At 12 weeks postgraft implantation, the gap at the injury site was bridged continuously. The collagen tube was absorbed and replaced by a tissue with a nerve-like appearance. There was no serious adhesion of the regenerated nerve to the surrounding tissue (Fig. 2D).

In vivo *collagen-binding assay*

We evaluated whether CBD-bFGF could be retained at the injury site of sciatic nerves. At 1, 4, 7, and 10 days after implantation, the LOCS was lysed and assessed by ELISA. As shown in Supplementary Fig. S2, the concentration of bFGF in the LOCS + CBD-bFGF group was significantly higher than that in the LOCS + PBS group, which indicated that CBD-bFGF was retained and enriched at the injury site ($n = 3$, $p < 0.05$). On day 10, although the average level in the LOCS + CBD-bFGF group was highest, there were no significant differences among the three grafted groups.

Walking track analysis

The SFI value ranged from −100, representing a complete loss of nerve function, to 0, representing normal nerve function. Before week 4, there were no significant differences among the three grafted groups. From week 5, the SFI value exhibited significant differences among the three grafted groups; functional recovery in the LOCS + NAT-bFGF group was superior to that in the LOCS + PBS group, but inferior to that in the LOCS + CBD-bFGF group ($n = 5$, $p < 0.05$) (Fig. 3).

Electrophysiological evaluation

We noted that the operated rats in each group showed different levels of recovery at week 12. The NCV in the LOCS + CBD-bFGF group and LOCS + NAT-bFGF group showed significant restoration compared with the LOCS + PBS group. In addition, there was a significant difference between the LOCS + CBD-bFGF group and LOCS + NAT-bFGF group ($n = 6$, $p < 0.01$) (Fig. 4A). The results of ACMAP were similar to those of NCV, but the difference between the CBD-bFGF group and NAT-bFGF group was not statistically significant ($n = 6$, $p > 0.05$) (Fig. 4B).

FG retrograde labeling

At week 12 after injury, FG-labeled sensory neurons in the DRG showed a golden color under UV irradiation (Fig. 5A). The labeled cells were recorded for each group. The group treated with LOCS + CBD-bFGF exhibited a significantly better sensory nerve fiber recovery compared with the LOCS + NAT-bFGF group and LOCS + PBS group. The number of labeled cells was higher in the LOCS + NAT-bFGF group than the LOCS + PBS group ($n = 4$, $p < 0.05$) (Fig. 5B).

Histological and morphometric analyses of regenerated nerves

HE staining indicated that the regenerated nerves guided by LOCS in the three grafted groups (LOCS + CBD-bFGF

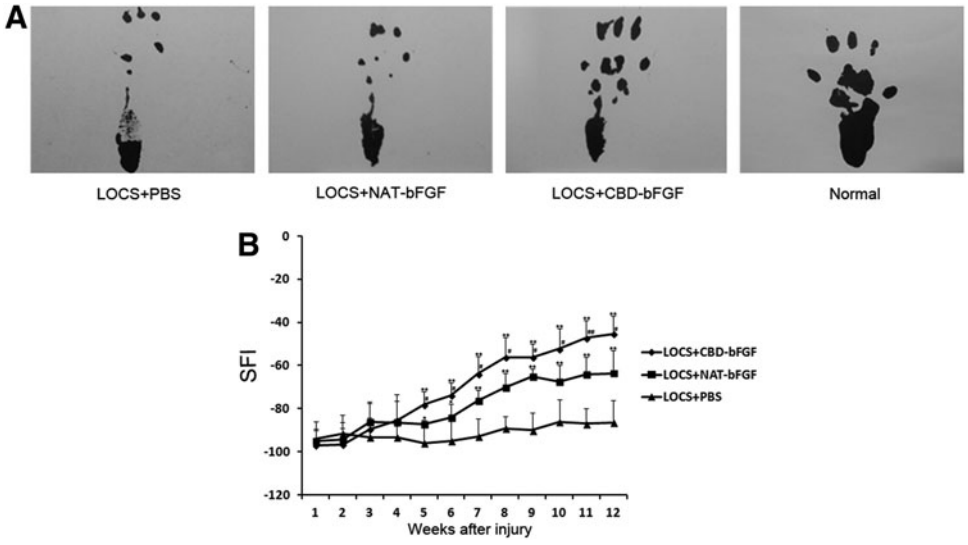

FIG. 3. Functional recovery was evaluated by walking track analysis. **(A)** Photographs of the rats' walking track prints in each group at 12 weeks following implantation. **(B)** Graph of sciatic function index (SFI) value of rats in the three grafted groups each week after injury. $^{\#}p < 0.05$, $^{\#\#}p < 0.01$, LOCS + CBD-bFGF group versus LOCS + NAT-bFGF group; $^{*}p < 0.05$, $^{**}p < 0.01$, LOCS + CBD-bFGF and LOCS + NAT-bFGF groups versus LOCS + PBS group. The data are expressed as mean ± SD, $n = 5$. SFI, sciatic function index.

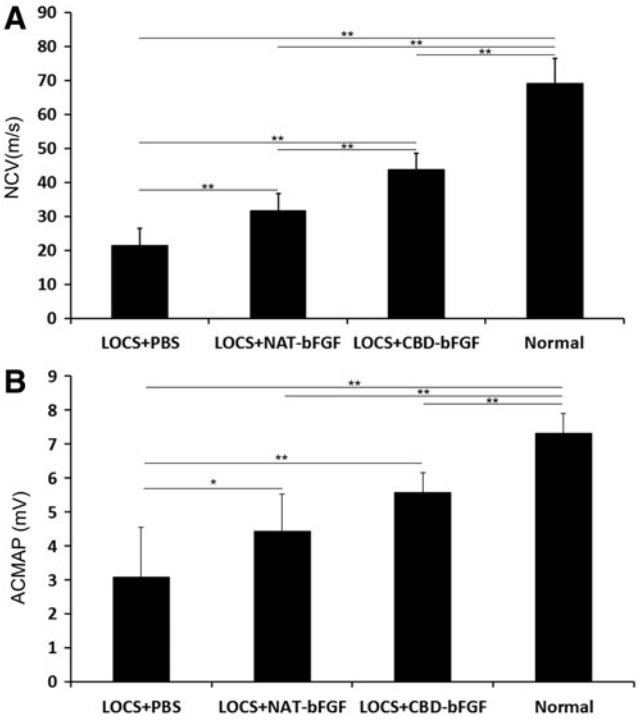

FIG. 4. Electrophysiological evaluation. **(A)** Nerve conduction velocity was detected at the injured side in the four groups 12 weeks after nerve grafting. **(B)** Amplitude of the compound muscle action potential (ACMAP) was determined at the injured side for the four groups 12 weeks after nerve grafting. The data are expressed as mean ± SD, $n = 6$, $^*p < 0.05$, $^{**}p < 0.01$. NCV, nerve conduction velocity.

group, LOCS + NAT-bFGF group, and LOCS + PBS group) exhibited a good, linear ordered structure (Fig. 6A).

To evaluate the density and distribution of axons in the regenerated nerve, transverse sections were stained with the anti-NF antibody (Fig. 6B). The LOCS + CBD-bFGF group had the best axonal recovery, while the LOCS + PBS group had an only sparsely NF-positive area at weeks 6 and 12 after injury. The differences among the three grafted groups were statistically significant ($n = 6$, $p < 0.05$) (Fig. 6D).

S-100 staining was used to assess the proliferation of Schwann cells, which is important for the successful axonal regeneration after injury (Fig. 6C). The S-100-positive area in the LOCS + CBD-bFGF group was significantly higher than those in the LOCS + NAT-bFGF and LOCS + PBS groups at weeks 6 and 12. Moreover, the S-100-positive area in the LOCS + NAT-bFGF group was significantly higher than that in the LOCS + PBS group ($n = 6$, $p < 0.01$) (Fig. 6E).

Analysis of regenerating cables

After staining of transverse sections with Luxol fast blue, the number and diameter of regenerated myelinated fibers were evaluated (Fig. 7A). The number and diameter of regenerated myelinated fibers exhibited increased progressively in the following order: LOCS + PBS group, LOCS + NAT-bFGF group, and LOCS + CBD-bFGF group at weeks 6 and 12, although the difference between the LOCS + NAT-bFGF group and LOCS + PBS group at week 6 was not statistically significant ($n = 5$, $p > 0.05$) (Fig. 7B, C).

The thickness of regenerated myelin sheaths was measured by TEM (Fig. 7D). The myelin sheaths in the LOCS + NAT-bFGF group were significantly thicker than those in the LOCS + PBS group, but thinner than those in the LOCS + CBD-bFGF group at weeks 6 and 12 ($n = 5$, $p < 0.05$) (Fig. 7E).

Muscle mass measurement and Masson's trichrome staining

An atrophic muscle can be alleviated upon reinnervation. Thus, gastrocnemius muscles were subjected to muscle mass measurement and Masson's trichrome staining on week 12. The weight ratio was significantly higher in the LOCS + CBD-bFGF group than the LOCS + PBS group and LOCS + NAT-bFGF group ($p < 0.01$). However, there was

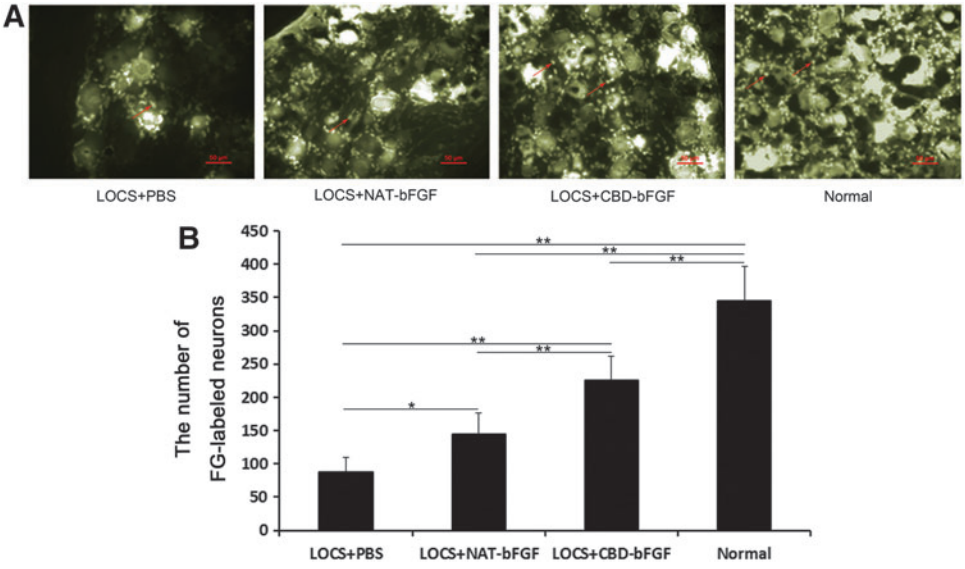

FIG. 5. FG retrograde tracing test at 12 weeks postimplantation. **(A)** The fluorogold (FG)-labeled neurons in the dorsal root ganglia (DRG) in the LOCS + PBS, LOCS + NAT-bFGF, and LOCS + CBD-bFGF groups compared with the normal group. The arrows indicate FG-labeled neurons. Scale bar, 50 μm. **(B)** The number of FG-labeled neurons was analyzed statistically. The data are expressed as mean ± SD, $n = 4$, $^*p < 0.05$, $^{**}p < 0.01$. Color images available online at www.liebertpub.com/tea

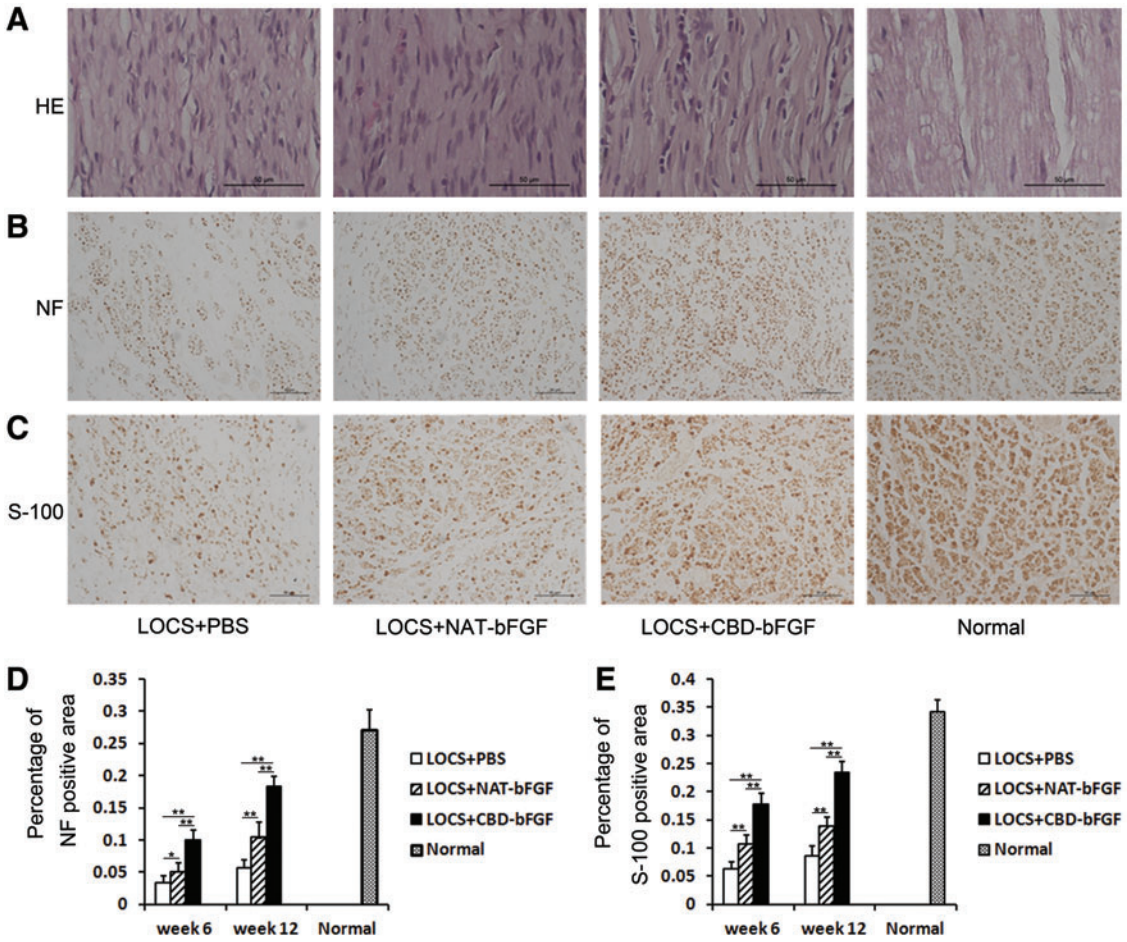

FIG. 6. Histological investigation and morphometric analysis at week 12 following implantation. **(A)** HE staining. Light micrographs of longitudinal sections in the four groups. Scale bar, 50 μm. **(B)** Immunostaining with anti-NF antibody. Light micrographs of the regenerating nerve cables. Scale bar, 50 μm. **(C)** Immunostaining with anti-S-100 antibody. Light micrographs of regenerating nerve cables. Scale bar, 50 μm. **(D)** Statistical analysis of the NF-positive area in each group. **(E)** Statistical analysis of the S-100-positive area in each group. The data are expressed as mean ± SD, $n = 6$, $^{*}p < 0.05$, $^{**}p < 0.01$. Color images available online at www.liebertpub.com/tea

no significant difference in the weight ratio between the LOCS + NAT-bFGF group and LOCS + PBS group ($n = 7$, $p > 0.05$) (Fig. 8B).

The percentage of muscle fiber-positive area was calculated (Fig. 8A). There were significant differences among the LOCS + PBS, LOCS + NAT-bFGF, and LOCS + CBD-bFGF groups. The percentage in the normal group was the highest, while that in the LOCS + PBS group was the lowest. The percentage in the LOCS + CBD-bFGF group was higher than that in the LOCS + NAT-bFGF group ($n = 6$, $p < 0.05$) (Fig. 8C).

Discussion

Various methods have been used to repair the peripheral nerve injury over the past several decades.[29–31] However, there is still no consensus regarding the most effective approach for regeneration of nerve defects. In this study, biological materials, that is, collagen tubes and LOCS, were applied for nerve regeneration. The collagen scaffolds showed good biocompatibility, while the linear ordered arrangement of the regenerated nerve fiber indicated that LOCS could guide the growth of regenerating nerve cables.

During the process of peripheral nerve regeneration, Schwann cells and axons in the proximal stump elongate into the biological materials and progress into the distal nerve stump.[32] However, using biological materials alone to repair the injured sciatic nerve is not effective. Many groups are now focusing on the molecular biological manipulation of internal features for nerve regeneration.[33] bFGF is important for the migration of Schwann cells,[34] and it also promotes neurite extension and stimulates Schwann cell proliferation. However, the effect of bFGF is often limited due to its rapid diffusion in the body fluids. In the present study, CBD-bFGF bound to the LOCS fibers was retained and enriched at the injury site (Supplementary Fig. S2), which enhanced peripheral nerve regeneration.

During the first week postimplantation, the SFI value decreased markedly to the lowest level in all grafted groups, which indicated that the surgery was successful. The NCV value could reflect the maturation of the regenerated fibers associated with the axonal diameter and myelination

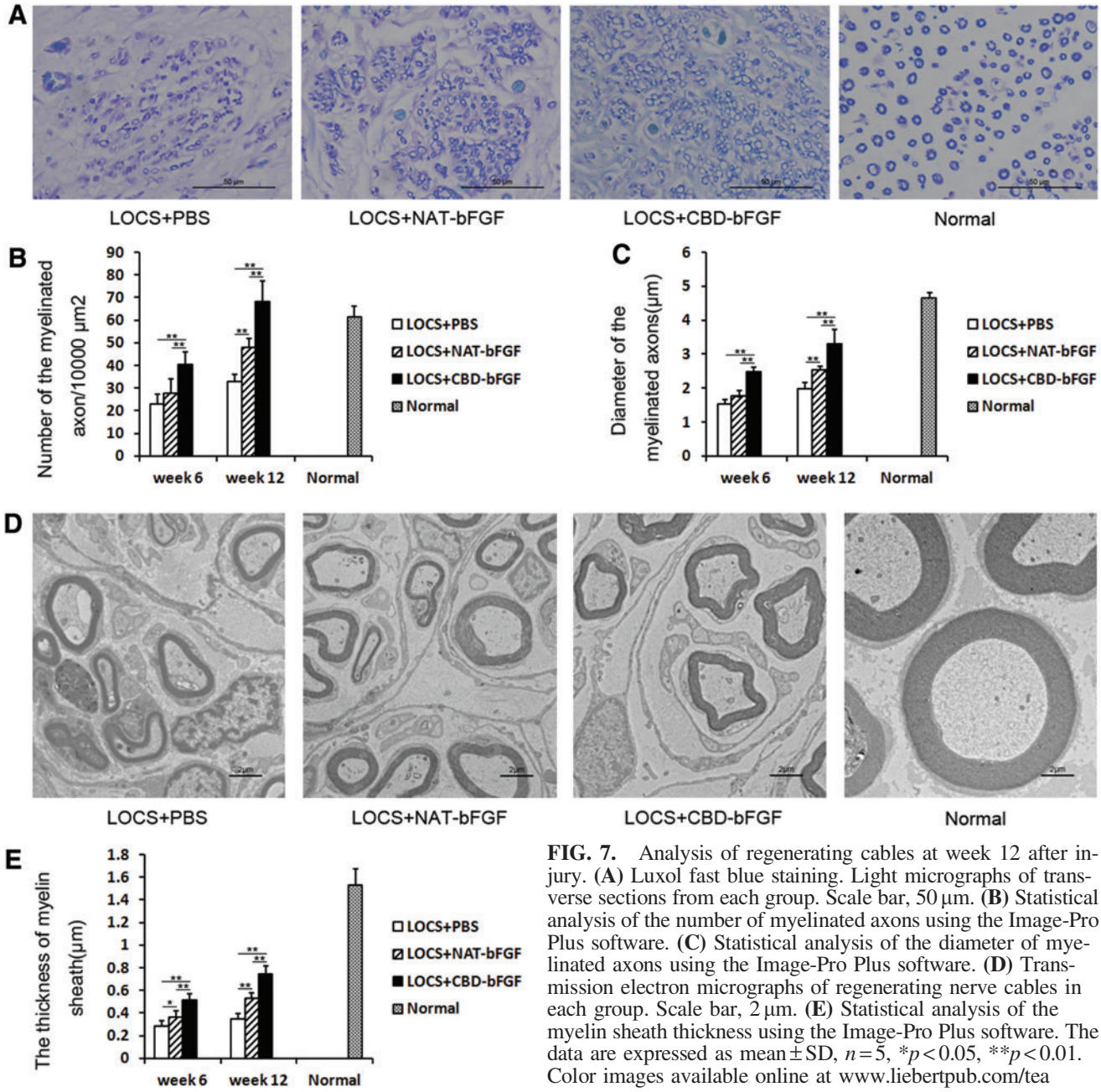

FIG. 7. Analysis of regenerating cables at week 12 after injury. **(A)** Luxol fast blue staining. Light micrographs of transverse sections from each group. Scale bar, 50 μm. **(B)** Statistical analysis of the number of myelinated axons using the Image-Pro Plus software. **(C)** Statistical analysis of the diameter of myelinated axons using the Image-Pro Plus software. **(D)** Transmission electron micrographs of regenerating nerve cables in each group. Scale bar, 2 μm. **(E)** Statistical analysis of the myelin sheath thickness using the Image-Pro Plus software. The data are expressed as mean ± SD, $n = 5$, $^{*}p < 0.05$, $^{**}p < 0.01$. Color images available online at www.liebertpub.com/tea

thickness, and ACMAP is directly proportional to the number of nerve fibers innervating the target muscle.[35] Retrograde labeling was performed to evaluate the number of sensory neurons that had sent axons across the graft. A positive correlation was observed between the number of labeled cells and the number of regenerated sensory nerve fibers.[36] The functional results in terms of SFI value, NCV, and the number of labeled sensory neurons showed that the LOCS + CBD-bFGF group recovered to a greater degree than the other two grafted groups. However, although the average ACMAP in the LOCS + CBD-bFGF group was higher than that in the LOCS + NAT-bFGF group, the difference was not statistically significant. This may have been due to the relatively high individual variation and the relatively small number of rats in each group in this study. Histological analyses of the regenerated nerve and target muscle were performed; the results were consistent with the functional evaluation.

Application of CBD-bFGF showed a significant regeneration effect in this study, probably because (1) CBD-bFGF could promote regeneration of the sciatic nerve after injury, and (2) CBD-bFGF could bind specifically to LOCS, thus achieving an effective concentration at the injury site. Most current strategies used to deliver bFGF are impractical for clinical use. Local injection of bFGF may result in rapid diffusion, increasing both the side effects and cost.[37] Applying genetically modified cells[38] or recombinant adeno-associated virus vectors[39] may cause immunological rejection.

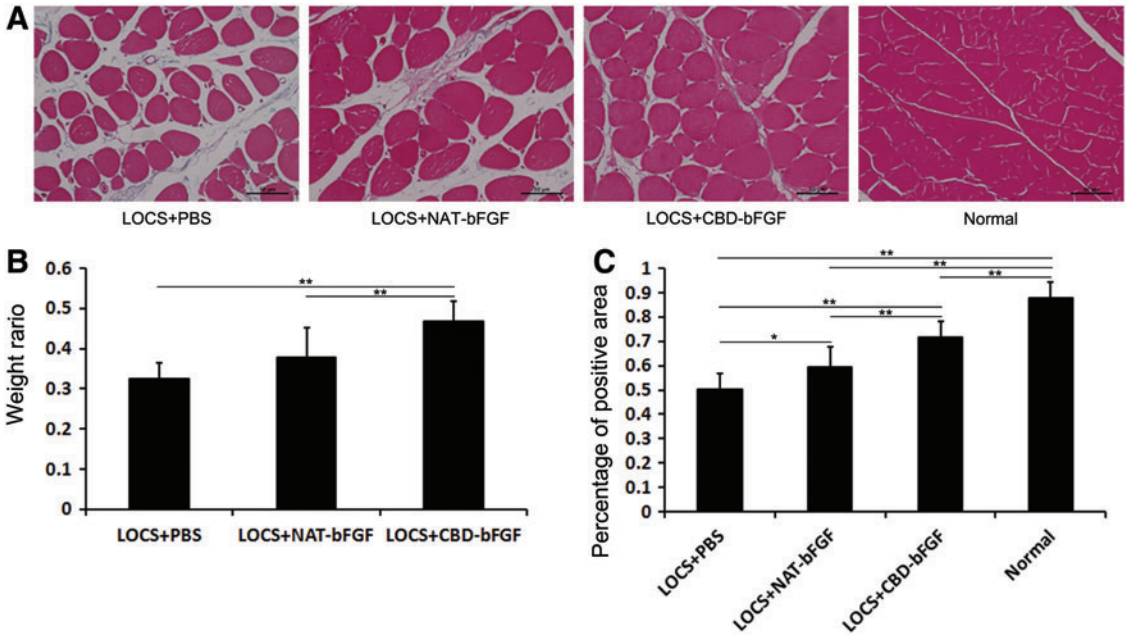

FIG. 8. Measurement of gastrocnemius muscle at 12 weeks after surgery. **(A)** Transverse sections of the gastrocnemius muscle following Masson's trichrome staining in each group. Scale bar, 50 μm. **(B)** The wet weight ratios of gastrocnemius muscle (injured side/uninjured side) for the three grafted groups. The data are expressed as mean ± SD, $n = 7$, $*p < 0.05$, $**p < 0.01$. **(C)** Statistical analysis of the muscle-positive area in transverse sections from each group. The data are expressed as mean ± SD, $n = 6$, $*p < 0.05$, $**p < 0.01$. Color images available online at www.liebertpub.com/tea

Infusion with an osmotic pump poses the risk of infection.[40] Some materials, such as fibrin gels, have low affinity for bFGF and covalent conjugation methods may cause safety problems.[23,41,42] In the present study, the use of CBD-bFGF enabled bFGF conjugation through mild reactions without the loss of its biological activity and required no toxic reagents. This is in marked contrast to the case of covalent conjugation through conventional condensation reactions.

Conclusions

In this study, synergistic effects were noted when collagen tubes and LOCS were used in combination with engineered bFGF as a natural biological functional scaffold to bridge a 5-mm gap in the rat sciatic nerve transection model. The LOCS fibers could guide the direction of nerve regeneration. CBD-bFGF loaded on the collagen scaffolds was retained and enriched at the injury site compared with NAT-bFGF, and promoted nerve regeneration and functional recovery. The use of natural, biological functional scaffolds represents a promising approach to the regeneration of peripheral nerve defects.

Acknowledgments

This work was supported by the National High Technology Research and Development Program (''863'' Program) of China (2012AA020501), the Military Medical Project (BWS11J002), the National Natural Science Foundation of China (30930032), and the ''Strategic Priority Research Program of the Chinese Academy of Sciences'' (Grant No. XDA01030401).

Disclosure Statement

No competing financial interests exist.

References

1. Noble, J., Munro, C.A., Prasad, V.S., and Midha, R. Analysis of upper and lower extremity peripheral nerve injuries in a population of patients with multiple injuries. J Trauma **45,** 116, 1998.
2. Korompilias, A.V., Payatakes, A.H., Beris, A.E., Vekris, M.D., Afendras, G.D., and Soucacos, P.N. Sciatic and peroneal nerve injuries. Microsurgery **26,** 288, 2006.
3. Kline, D.G., Kim, D., Midha, R., Harsh, C., and Tiel, R. Management and results of sciatic nerve injuries: a 24-year experience. J Neurosurg **89,** 13, 1998.
4. Lundborg, G., Dahlin, L.B., Danielsen, N., Gelberman, R.H., Longo, F.M., Powell, H.C., *et al.* Nerve regeneration in silicone chambers: influence of gap length and of distal stump components. Exp Neurol **76,** 361, 1982.
5. Seckel, B.R., Chiu, T.H., Nyilas, E., and Sidman, R.L. Nerve regeneration through synthetic biodegradable nerve guides: regulation by the target organ. Plast Reconstr Surg **74,** 173, 1984.
6. Tang, X., Xue, C., Wang, Y., Ding, F., Yang, Y., and Gu, X. Bridging peripheral nerve defects with a tissue engineered nerve graft composed of an *in vitro* cultured nerve equivalent and a silk fibroin-based scaffold. Biomaterials **33,** 3860, 2012.
7. Jiang, M., Zhuge, X., Yang, Y., Gu, X., and Ding, F. The promotion of peripheral nerve regeneration by chitooligosaccharides in the rat nerve crush injury model. Neurosci Lett **454,** 239, 2009.

8. Ghasemi-Mobarakeh, L., Prabhakaran, M.P., Morshed, M., Nasr-Esfahani, M.H., and Ramakrishna, S. Electrospun poly(epsilon-caprolactone)/gelatin nanofibrous scaffolds for nerve tissue engineering. Biomaterials **29,** 4532, 2008.
9. Hudson, T.W., Liu, S.Y., and Schmidt, C.E. Engineering an improved acellular nerve graft via optimized chemical processing. Tissue Eng **10,** 1346, 2004.
10. Boccafoschi, F., Habermehl, J., Vesentini, S., and Mantovani, D. Biological performances of collagen-based scaffolds for vascular tissue engineering. Biomaterials **26,** 7410, 2005.
11. Chamberlain, L.J., Yannas, I.V., Hsu, H.P., Strichartz, G., and Spector, M. Collagen-GAG substrate enhances the quality of nerve regeneration through collagen tubes up to level of autograft. Exp Neurol **154,** 315, 1998.
12. Li, X., Feng, Q., Liu, X., Dong, W., and Cui, F. Collagen-based implants reinforced by chitin fibres in a goat shank bone defect model. Biomaterials **27,** 1917, 2006.
13. Ju, Y.E., Janmey, P.A., McCormick, M.E., Sawyer, E.S., and Flanagan, L.A. Enhanced neurite growth from mammalian neurons in three-dimensional salmon fibrin gels. Biomaterials **28,** 2097, 2007.
14. Brushart, T.M., Mathur, V., Sood, R., and Koschorke, G.M., and Joseph, H. Boyes Award. Dispersion of regenerating axons across enclosed neural gaps. J Hand Surg Am **20,** 557, 1995.
15. Madison, R.D., Archibald, S.J., Lacin, R., and Krarup, C. Factors contributing to preferential motor reinnervation in the primate peripheral nervous system. J Neurosci **19,** 11007, 1999.
16. Hamilton, S.K., Hinkle, M.L., Nicolini, J., Rambo, L.N., Rexwinkle, A.M., Rose, S.J., *et al.* Misdirection of regenerating axons and functional recovery following sciatic nerve injury in rats. J Comp Neurol **519,** 21, 2011.
17. Lin, H., Chen, B., Wang, B., Zhao, Y., Sun, W., and Dai, J. Novel nerve guidance material prepared from bovine aponeurosis. J Biomed Mater Res A **79,** 591, 2006.
18. Han, Q., Sun, W., Lin, H., Zhao, W., Gao, Y., Zhao, Y., *et al.* Linear ordered collagen scaffolds loaded with collagen-binding brain-derived neurotrophic factor improve the recovery of spinal cord injury in rats. Tissue Eng Part A **15,** 2927, 2009.
19. Han, Q., Jin, W., Xiao, Z., Ni, H., Wang, J., Kong, J., *et al.* The promotion of neural regeneration in an extreme rat spinal cord injury model using a collagen scaffold containing a collagen binding neuroprotective protein and an EGFR neutralizing antibody. Biomaterials **31,** 9212, 2010.
20. Fujimoto, E., Mizoguchi, A., Hanada, K., Yajima, M., and Ide, C. Basic fibroblast growth factor promotes extension of regenerating axons of peripheral nerve. *In vivo* experiments using a Schwann cell basal lamina tube model. J Neurocytol **26,** 511, 1997.
21. Wang, S., Cai, Q., Hou, J., Bei, J., Zhang, T., Yang, J., *et al.* Acceleration effect of basic fibroblast growth factor on the regeneration of peripheral nerve through a 15-mm gap. J Biomed Mater Res A **66,** 522, 2003.
22. Grothe, C., Meisinger, C., and Claus, P. *In vivo* expression and localization of the fibroblast growth factor system in the intact and lesioned rat peripheral nerve and spinal ganglia. J Comp Neurol **434,** 342, 2001.
23. Ohta, M., Suzuki, Y., Chou, H., Ishikawa, N., Suzuki, S., Tanihara, M., *et al.* Novel heparin/alginate gel combined with basic fibroblast growth factor promotes nerve regeneration in rat sciatic nerve. J Biomed Mater Res A **71,** 661, 2004.
24. Rapraeger, A.C., Krufka, A., and Olwin, B.B. Requirement of heparan sulfate for bFGF-mediated fibroblast growth and myoblast differentiation. Science **252,** 1705, 1991.
25. de Souza, S.J., and Brentani, R. Collagen binding site in collagenase can be determined using the concept of sense-antisense peptide interactions. J Biol Chem **267,** 13763, 1992.
26. Zhao, W., Chen, B., Li, X., Lin, H., Sun, W., Zhao, Y., *et al.* Vascularization and cellularization of collagen scaffolds incorporated with two different collagen-targeting human basic fibroblast growth factors. J Biomed Mater Res A **82,** 630, 2007.
27. Yang, Y., Zhao, Y., Chen, B., Han, Q., Sun, W., Xiao, Z., *et al.* Collagen-binding human epidermal growth factor promotes cellularization of collagen scaffolds. Tissue Eng Part A **15,** 3589, 2009.
28. Bain, J.R., Mackinnon, S.E., and Hunter, D.A. Functional evaluation of complete sciatic, peroneal, and posterior tibial nerve lesions in the rat. Plast Reconstr Surg **83,** 129, 1989.
29. Chen, Z.W., and Wang, M.S. Effects of nerve growth factor on crushed sciatic nerve regeneration in rats. Microsurgery **16,** 547, 1995.
30. Pierucci, A., de Duek, E.A., and de Oliveira AL. Peripheral nerve regeneration through biodegradable conduits prepared using solvent evaporation. Tissue Eng Part A **14,** 595, 2008.
31. Hadlock, T., Sundback, C., Hunter, D., Cheney, M., and Vacanti, J.P. A polymer foam conduit seeded with Schwann cells promotes guided peripheral nerve regeneration. Tissue Eng **6,** 119, 2000.
32. Chen, Y.Y., McDonald, D., Cheng, C., Magnowski, B., Durand, J., and Zochodne, D.W. Axon and Schwann cell partnership during nerve regrowth. J Neuropathol Exp Neurol **64,** 613, 2005.
33. Pereira Lopes, F.R., Frattini, F., Marques, S.A., Almeida, F.M., de Moura Campos, L.C., Langone, F., *et al.* Transplantation of bone-marrow-derived cells into a nerve guide resulted in transdifferentiation into Schwann cells and effective regeneration of transected mouse sciatic nerve. Micron (Oxford, England: 1993) **41,** 783, 2010.
34. Han, H., Ao, Q., Chen, G., Wang, S., and Zuo, H. A novel basic fibroblast growth factor delivery system fabricated with heparin-incorporated fibrin-fibronectin matrices for repairing rat sciatic nerve disruptions. Biotechnol Lett **32,** 585, 2010.
35. Ding, T., Lu, W.W., Zheng, Y., Li, Z., Pan, H., and Luo, Z. Rapid repair of rat sciatic nerve injury using a nanosilver-embedded collagen scaffold coated with laminin and fibronectin. Regen Med **6,** 437, 2011.
36. Ding, F., Wu, J., Yang, Y., Hu, W., Zhu, Q., Tang, X., *et al.* Use of tissue-engineered nerve grafts consisting of a chitosan/poly(lactic-co-glycolic acid)-based scaffold included with bone marrow mesenchymal cells for bridging 50-mm dog sciatic nerve gaps. Tissue Eng Part A **16,** 3779, 2010.
37. Unger, E.F., Goncalves, L., Epstein, S.E., Chew, E.Y., Trapnell, C.B., Cannon, R.O., 3rd, *et al.* Effects of a single intracoronary injection of basic fibroblast growth factor in stable angina pectoris. Am J Cardiol **85,** 1414, 2000.

38. Fujiwara, K., Date, I., Shingo, T., Yoshida, H., Kobayashi, K., Takeuchi, A., *et al.* Reduction of infarct volume and apoptosis by grafting of encapsulated basic fibroblast growth factor-secreting cells in a model of middle cerebral artery occlusion in rats. J Neurosurg **99,** 1053, 2003.
39. Madry, H., Kohn, D., and Cucchiarini, M. Direct FGF-2 gene transfer via recombinant adeno-associated virus vectors stimulates cell proliferation, collagen production, and the repair of experimental lesions in the human ACL. Am J Sports Med **41,** 194, 2013.
40. Landau, C., Jacobs, A.K., and Haudenschild, C.C. Intrapericardial basic fibroblast growth factor induces myocardial angiogenesis in a rabbit model of chronic ischemia. Am Heart J **129,** 924, 1995.
41. Tabata, Y., and Ikada, Y. Vascularization effect of basic fibroblast growth factor released from gelatin hydrogels with different biodegradabilities. Biomaterials **20,** 2169, 1999.
42. DeLong, S.A., Moon, J.J., and West, J.L. Covalently immobilized gradients of bFGF on hydrogel scaffolds for directed cell migration. Biomaterials **26,** 3227, 2005.

Address correspondence to:
Jianwu Dai, PhD
State Key Laboratory of Trauma,
Burns and Combined Injury
Chongqing Engineering Research Center for Nanomedicine
Institute of Combined Injury
College of Preventive Medicine
Third Military Medical University
30, Gaotanyan Road
Chongqing 400038
China

E-mail: jwdai@genetics.ac.cn

Ruxiang Xu, PhD
The Affiliated Bayi Brain Hospital
The Military General Hospital of Beijing PLA
No.5 Nanmen Cang, Dongcheng District
Beijing 100700
China

E-mail: zjxuruxiang@163.com

Received: March 5, 2013
Accepted: November 1, 2013
Online Publication Date: March 13, 2014